JACS
JOURNAL OF THE AMERICAN CHEMICAL SOCIETY

ARTICLE

pubs.acs.org/JACS

A Powerful Approach for the Selection of 2-Aminopurine Substitution Sites to Investigate RNA Folding

Marie F. Soulière, Andrea Haller, Renate Rieder,[†] and Ronald Micura*

Institute of Organic Chemistry, Center for Molecular Biosciences Innsbruck (CMBI), University of Innsbruck, Innrain 52a, 6020 Innsbruck, Austria

Supporting Information

ABSTRACT: A precise tertiary structure must be adopted to allow the function of many RNAs in cells. Accordingly, increasing resources have been devoted to the elucidation of RNA structures and the folding of RNAs. 2-Aminopurine (2AP), a fluorescent nucleobase analogue, can be substituted in strategic positions of DNA or RNA molecules to act as site-specific probe to monitor folding and folding dynamics of nucleic acids. Recent studies further demonstrated the potential of 2AP modifications in the assessment of folding kinetics during ligand-induced secondary and tertiary RNA structure rearrangements. However, an efficient way to unambiguously identify reliable positions for 2AP sensors is as yet unavailable and would represent a major asset, especially in the absence of crystallographic or NMR structural data for a target molecule. We report evidence of a novel and direct correlation between the 2′-OH flexibility of nucleotides, observed by selective 2′-hydroxyl acylation analyzed by primer extension (SHAPE) probing and the fluorescence response following nucleotide substitutions by 2AP. This correlation leads to a straightforward method, using SHAPE probing with benzoyl cyanide, to select appropriate nucleotide sites for 2AP substitution. This clear correlation is presented for three model RNAs of biological significance: the SAM-II, adenine (addA), and preQ$_1$ class II (preQ$_1$cII) riboswitches.

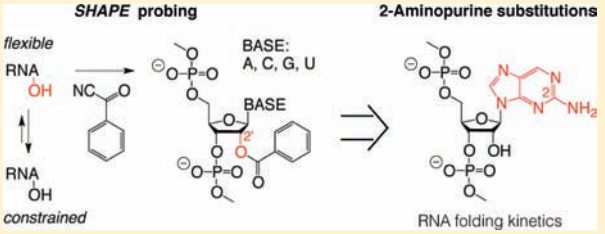

INTRODUCTION

RNA molecules are known to play a critical role in cells in the catalysis of biological reactions, the control of gene expression, and the response to internal or external stimuli.[1−7] For many RNAs, such as transfer RNAs (tRNAs), ribozymes, and riboswitches, a precise tertiary structure must be adopted to allow their function.[8−10] Accordingly, in the past decade, increasing resources have been devoted to the elucidation of RNA structures and the folding of RNAs.

The 2-aminopurine base (2AP), a fluorescent nucleobase, has been used as a site-specific probe to monitor local structural changes in nucleic acids.[11,12] Base stacking of 2AP is known to quench its fluorescence emission in a quantifiable manner.[11] Since the modified base can interact with thymine/uracil in a Watson−Crick geometry or with cytosine in a wobble configuration,[13,14] it can be substituted in strategic positions of an RNA molecule to address the basic folding and folding dynamics of RNA structures. While previously mainly used to monitor oligonucleotides duplex formation, recent studies demonstrated the potential of 2AP modifications in the assessment of folding kinetics during ligand-induced secondary and tertiary RNA structure rearrangements.[15−22] In particular, the 2AP-based RNA folding analysis (2APfold, recently reviewed in ref 23) can provide a time order for the structure formation of the various segments within an RNA molecule,[17−20] hard to obtain by any other method. However, especially in the absence of crystallographic or NMR structural data, the selection of proper 2AP labeling positions to investigate RNA folding kinetics can be a fastidious task, not least because 2AP modification requires chemical synthesis and enzymatic ligation to achieve these RNA derivatives. Therefore, an efficient way to unambiguously identify reliable positions for 2AP sensors would represent a major asset.

On the other hand, selective 2′-hydroxyl acylation analyzed by primer extension (SHAPE) is a method currently in use to probe simultaneously the secondary and tertiary nucleobase interactions of all nucleotides within RNA molecules.[24−26] It takes advantage of the nucleophilicity of the ribose 2′-OH in unconstrained nucleotides, allowing electrophiles, such as *N*-methylisatoic anhydride (NMIA) or benzoyl cyanide (BzCN), to form 2′-O-adducts according to the local flexibility of the nucleotide position. Nucleotides involved in Watson−Crick (C:G, A:U) or noncanonical but stable base pairing (U:G, A:A, A:G) will therefore present less flexibility and reactivity to the SHAPE reagent.[27] Reverse transcription on the modified RNA permits a quantifiable detection of the 2′-OH reactivity for whole RNA molecules.[25,28]

A correlation between SHAPE chemistry and the generalized NMR order parameter S^2 has been previously reported[29] highlighting the fact that SHAPE probing monitors spatial disorder and structural dynamics. In the current study, we sought to investigate whether the spatial disorder data obtained from SHAPE

Received: July 8, 2011
Published: September 01, 2011

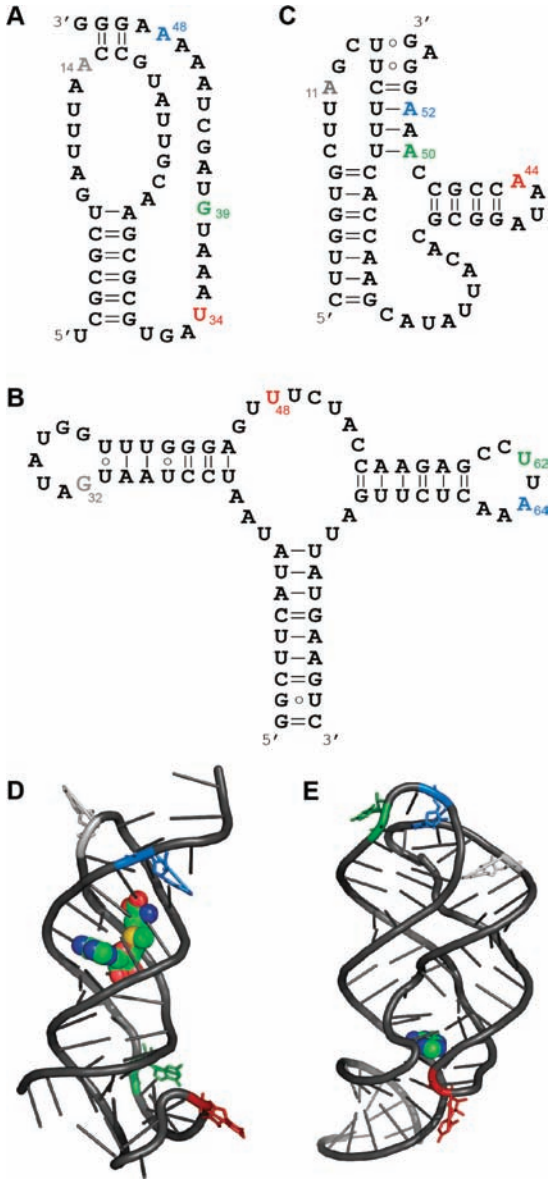

Figure 1. RNA structures and 2AP substitution sites. Basic secondary structure representations for the SAM-II (a), addA (b), and preQ1cII (c) riboswitches and crystallographic tertiary structures for the SAM-II (d) (2QWY) and addA (e) (PDB 1Y26) riboswitches. The 2AP substitution sites utilized for the upcoming figures are numbered and presented in their respective colors in the next figures (gray, red, green, and blue).

probing could predict adequate substitution positions for 2AP-based RNA folding experiments. We report evidence of a novel and direct correlation between the 2′-OH flexibility of nucleotides, observed by SHAPE probing, and the fluorescence response following nucleotide substitutions by 2AP. This correlation leads to a straightforward method, using SHAPE probing with BzCN, to select appropriate nucleotide sites for 2AP substitution on a RNA target, especially in the absence of crystallographic or NMR structural data. This clear correlation is presented for two model RNAs: the SAM-II and adenine (addA) riboswitches (Figure 1). A third RNA of biological significance, the preQ$_1$ class II (preQ$_1$cII) riboswitch, is used to demonstrate the validity of the method (Figure 1).

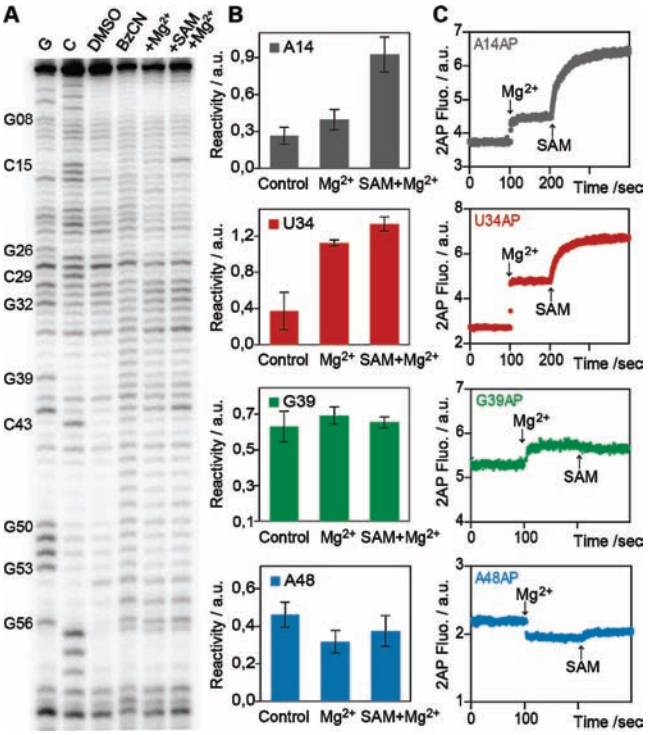

Figure 2. Correlation between SHAPE probing and 2AP fluorescence for the SAM-II riboswitch. (a) Typical gel for the probing of the SAM-II RNA structure with BzCN. Lanes from left to right: G and C bases ladders, control in the absence of probing reagent, probing with BzCN, probing in the presence of 2 mM of $MgCl_2$, probing in the presence of 2 mM of $MgCl_2$, and 5 μM of SAM. (b) Relative 2′-OH reactivity for four selected bases of the SAM-II riboswitch obtained from quantification and normalization of the SHAPE probing results, and (c) 2AP fluorescence observed for the corresponding bases, upon injection of 2 mM of $MgCl_2$ followed by 5 μM of SAM.

RESULTS AND DISCUSSION

Confirmation of SHAPE Probing of the SAM-II Riboswitch. SHAPE probing of the SAM-II RNA was first undertaken using the BzCN reagent. While SHAPE data is already available for this riboswitch, the probing was assessed with a different acylation agent, NMIA, in the presence of magnesium and SAM ligand.[30] We wished to produce additional data on the magnesium-dependent folding, which was not explored by this experiment in previous studies. We therefore probed the structure of the SAM-II riboswitch in the presence and absence of 2 mM of $MgCl_2$, with or without 5 μM of SAM ligand (Figure 2A). The results were normalized according to the efficiency of the reverse transcription, and the background in the absence of acylation agent was further subtracted. The mean of at least two separate experiments is presented in Figure 2B and Supporting Figure 1E, Supporting Information. It has to be kept in mind that the intensity of a band on the sequencing gel represents the degree of 2′-hydroxyl acylation of the following base during reverse transcription, which corresponds to the previous base in the primary RNA sequence. The variation between the different states was also calculated for the bases utilized for 2AP substitutions, and these data are presented in Table 1.

As previously shown by Gilbert et al.,[30] a strong protection of the SAM binding pocket, corresponding to residues G8-U12, A19-A24, G42-C43, A45-A47, is observable by SHAPE probing

Table 1. Correlation Between SHAPE Probing and 2AP Fluorescence Data[a]

		relative probing[b]		relative fluorescence[b]	
riboswitch	nucleotide	+ Mg^{2+}	+ Mg^{2+} + ligand	+ Mg^{2+}	+ Mg^{2+} + ligand
SAM-II	A14	1.50	3.52	1.22	1.73
	U34	3.04	3.61	1.67	2.55
	G39	1.10	1.04	1.07	1.04
	A48	0.689	0.811	0.90	0.95
addA	G32	0.556	0.170	0.742	0.604
	U48	1.23	3.04	1.16	3.54
	U62	1.61	1.41	1.63	1.62
	A64	0.342	0.125	0.780	0.734
$preQ_1$cII	A11	1.36	3.64	1.00	1.51
	A44	0.972	0.110	0.920	0.889
	A50	1.07	12.5	1.20	1.21
	A52	0.460	0.193	0.862	0.821

[a] For complete data set and errors, see Supporting Table 1, Supporting Information. [b] Initial state of the riboswitches without ligands is defined to have a value of 1.

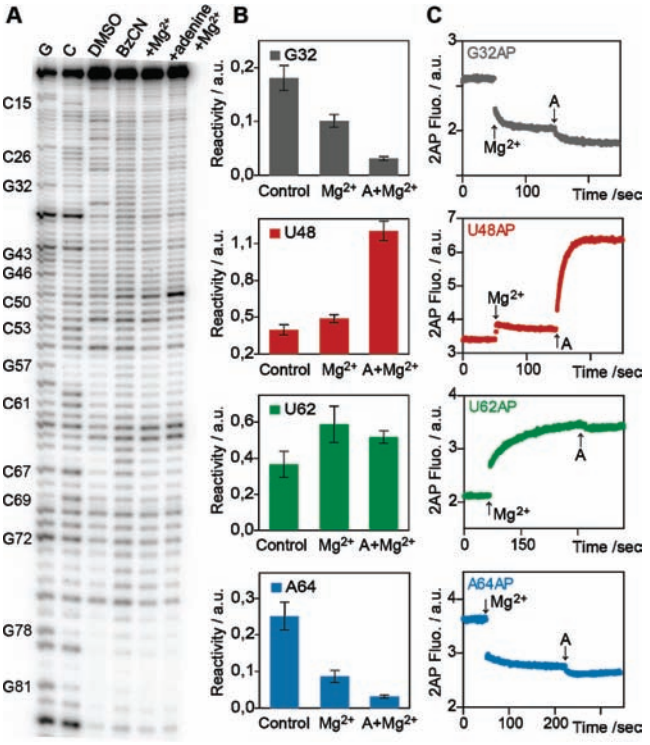

Figure 3. Correlation between SHAPE probing and 2AP fluorescence for the adenine riboswitch. (a) Typical gel for the probing of the addA RNA structure with BzCN. Lanes from left to right: G and C bases ladders, control in the absence of probing reagent, probing with BzCN, probing in the presence of 2 mM of $MgCl_2$, probing in the presence of 2 mM of $MgCl_2$, and 10 μM of adenine (A). (b) Relative 2′-OH reactivity for four selected bases of the addA riboswitch obtained from quantification and normalization of the SHAPE probing results, and (c) 2AP fluorescence observed for the corresponding bases, upon injection of 2 mM of $MgCl_2$ followed by 10 μM of adenine (A).

in the presence of ligand (Figure 2A and Supporting Figure 1E, Supporting Information). In contrast, nucleotides A14, U34 and A41 present a very significant increase in reactivity with the BzCN reagent upon SAM ligand addition, comparable to what was detected using NMIA.[30] We further demonstrate that these latter effects can also be observed in the presence of sole magnesium, although to a lower extent. This suggests that magnesium ions are contributing to the folding of the riboswitch to generate a SAM-binding competent structure, as recently demonstrated by single-molecule FRET and 2AP kinetics studies.[20] It can also be observed that while a decrease in reactivity is measured for bases U18 and A49 in the presence of SAM ligand and magnesium, with magnesium alone, these two bases become more accessible to acylation, suggesting that these bases first undergo a destabilization or unstacking before reaching a final less flexible conformation upon SAM binding to the riboswitch (Figure 2A and Supporting Figure 1E, Supporting Information). Additionally, the probing in the absence of magnesium and ligand demonstrates that the pseudoknot does not appear to be forming in this condition, as also evidenced by recent smFRET data on the SAM-II riboswitch.[20]

Noteworthily, if we compare the reactivity in the presence of magnesium ions alone and with further addition of SAM, the results obtained in the current study with BzCN (Figure 2A and Supporting Figure 1E, Supporting Information) are in agreement with previous data reported with the NMIA reagent.[30]

These SHAPE results were compared with the 2AP fluorescence from modifications at six distinct positions within the SAM-II RNA (Figure 1A and Supporting Figure 1A, B, and E, Supporting Information), upon injection of 2 mM $MgCl_2$, followed by 5 μM SAM ligand (Figure 2C and Supporting Figure 1C, D, and E, Supporting Information). The 2AP substitution positions were selected using the crystallographic data of the SAM-II riboswitch (Figure 1D).[20,30] The fluorescence variation for the 2AP substitutions was monitored as a function of time, and the results were quantified as the relative fluorescence variation between the plateaus (Table 1 and Supporting Table 1, Supporting Information).

Comparison of the SHAPE and 2AP results supports that every decrease in 2AP fluorescence upon each ligand interaction (Mg^{2+} and SAM) with the SAM-II RNA also resulted in a similar decrease in 2′-OH flexibility, observed by BzCN probing. The same correlation can be observed for increases in fluorescence and 2′-OH acylation levels and with diverging effects from magnesium ions and SAM interactions (for example, increased fluorescence upon magnesium addition, followed by decrease when the SAM ligand is added to the mixture) (Figure 2B and C). Noteworthy, while the BzCN probing results include a background subtraction, this is not the case for the 2AP substitution data, resulting in values that are not strictly comparable. Nonetheless, we quantified the correlation between SHAPE probing and 2AP fluorescence by calculating the Pearson correlation coefficient (r). This coefficient reflects the degree of linear relationship between two variables. Its value varies from 1 to −1, with 0 meaning that there is no linear relationship between the variables, while a value of 1 represents a perfect positive linear correlation. A strong positive correlation can be calculated from the data in the presence of magnesium ions, r = 0.76, as well as in the presence of magnesium and SAM, r = 0.66, for the SAM-II riboswitch. These positive coefficients underline the fact that

high SHAPE values are associated with high 2AP fluorescence values.

It is also important to point out that among the six bases presenting the highest variation in SHAPE reactivity between the different conditions (U1, A14, G30, U31, U34, and A41) (Supporting Figure 1E, Supporting Information) can be found in the three bases recently selected to monitor the folding rate kinetics parameters of the SAM-II riboswitch (A14, U34, A41).[20] Large variations in SHAPE reactivity therefore appear as a significant indicator of proportional extensive 2AP fluorescence variations in RNA molecules, which are required to monitor effective kinetics parameters.

Probing of the addA Riboswitch. To further support the hypothesis of direct correlation between SHAPE probing and 2AP fluorescence, SHAPE probing experiments were performed on a second RNA molecule with existing 2AP and crystallographic data, the addA riboswitch from *Vibrio vulnificus*.[18,31] In this case, the fluorescence data for 15 positions previously selected for 2AP analysis of the addA riboswitch[18,32] (Figure 1B and E and Supporting Figure 2A and B and Table 1, Supporting Information) were compared to novel SHAPE probing on the same RNA sequence. The probing experiments were performed with the magnesium and adenine ligand concentrations utilized for the 2AP experiments: 2 mM and 10 μM, respectively. Clear changes in 2′-OH flexibility were observed in the probing pattern with BzCN between the different conditions (Figure 3A and Supporting Figure 2G, Supporting Information), including an increased 2′-OH flexibility of uridines 48 and 62 and a marked decrease for A24, U31, A35, G38, A64, and U75.

Formation of the global fold of the tuning fork-like aptamer structure can be observed in the presence of sole magnesium. The SHAPE band intensities of the individual nucleotides involved in the loop−loop interaction (34−38, 60−65) are drastically affected in response to the metal ions, highlighting the initial preorganization of this long-range interaction without adenine. In response to both magnesium and adenine, the band intensities are affected further, whereby the contribution stemming from adenine binding was generally smaller compared to the contribution stemming from magnesium ions. This indicates that the regions distant from the binding site become further rigidified upon ligand binding (Figure 3A and Supporting Figure 2G, Supporting Information). As observed in the three-dimensional structure of the addA riboswitch,[31] base U48 becomes completely unstacked and solvent accessible in the presence of adenine. Only nucleotides U47 and U62 were also observed to have an overall increased 2′-OH reactivity upon magnesium and adenine addition. All the other nucleotides of the sequence possess a decreased flexibility in the presence of both ligands (Figure 3A and Supporting Figure 2G, Supporting Information).

A direct correlation can be observed between the SHAPE probing results and the 2AP fluorescence data for the addA riboswitch (Figure 3C and Supporting Figure 2C−F, Supporting Information). Quantification of the variation between the different binding states is available in Table 1 and Supporting Table 1, Supporting Information and highlights the correlation between the effect of magnesium and adenine addition on the riboswitch measured by both 2AP fluorescence and 2′-hydroxyl acylation by BzCN. As observed for the SAM-II riboswitch, the direction of the effect is conserved for all 15 tested nucleotides for both ligands effects. Correlation coefficients r of 0.86 and 0.97 were respectively obtained from the data in the presence of sole magnesium and with added adenine ligand, highlighting the presence of a strong positive correlation between the results from the two techniques.

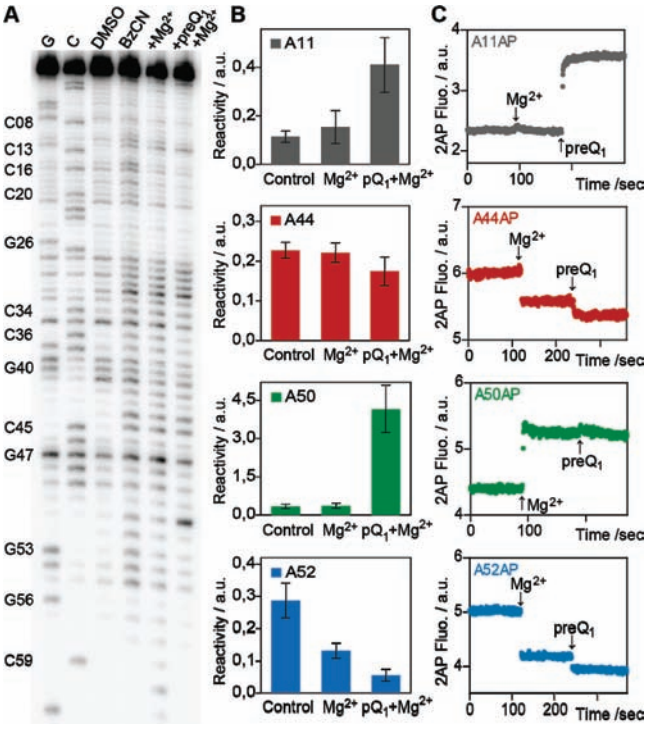

Figure 4. Correlation between SHAPE probing and 2AP fluorescence for the preQ$_1$cII riboswitch. (a) Typical gel for the probing of the preQ$_1$cII RNA structure with BzCN. Lanes from left to right: G and C bases ladders, control in the absence of probing reagent, probing with BzCN, probing in the presence of 5 mM of $MgCl_2$, probing in the presence of 5 mM of $MgCl_2$, and 10 μM of preQ$_1$. (b) Relative 2′-OH reactivity for four selected bases of preQ$_1$cII riboswitch obtained from quantification and normalization of the SHAPE probing results, and (c) 2AP fluorescence observed for the corresponding bases, upon injection of 4 mM of $MgCl_2$ followed by 10 μM of preQ$_1$.

Additionally, our research group previously published an analysis of the folding kinetics (2APfold) and association constants (K_D) for the addA riboswitch using 2AP substitutions, presenting the kinetics parameters of ligand interaction for bases A24, A35, G38, and U48.[18] Gilbert et al. also reported an association rate constant for 7-deazaguanine binding to the U48−2AP substitution in the *Bacillus subtilis* guanine riboswitch.[22] The addA A35, G38, and U48 are within the 10 most reactive bases detected here by BzCN probing of the addA riboswitch (5 of which are comprised in the loop 32−38) (Supporting Figure 2G, Supporting Information). While probing of base A24 in the presence of magnesium and adenine did not produce a variation in the range of the more reactive bases of the sequence, its reactivity was the highest within the short-loop region 21−25 and would be, only based on the SHAPE results, the substitution position of choice to monitor structural changes in this region.

SHAPE Probing and 2AP Substitution of the preQ$_1$cII Riboswitch. To strengthen the conclusions of the SHAPE—2AP correlation, we selected a third RNA, the preQ$_1$cII riboswitch,[33] for which no crystal structure is available to help with 2AP substitution position selection. We first performed SHAPE experiments in the absence and presence of 5 mM of magnesium, with or without 10 μM of preQ$_1$ ligand (Figure 4A and B and Supporting Figure 3C, Supporting Information). The probing

demonstrated that the preformation of the pseudoknot (14−19, 50−56) occurs upon addition of magnesium and that this interaction is further stabilized by $preQ_1$ binding, with the exception of base A50, which becomes unstacked in the presence of $preQ_1$ ligand. The free loops 26−36 and 40−44 become increasingly flexible with ligand addition, while the nucleotides in loop 8−13 present various reactions to ligands, with base A11 being the only one to become clearly more increasingly flexible with the sequential addition of magnesium and $preQ_1$.

The latter results led to the selection of five substitution positions for 2AP according to their observed flexibility (Figure 4A and Supporting Figure 3C, Supporting Information). All the selected nucleotides, A11, G12, A44, A50, and A52, presented strong flexibility variations in SHAPE probing, suggesting that they could be an interesting substitution position for 2AP experiments (Table 1 and Supporting Table 1, Supporting Information). First, position A52 was selected to observe the folding of the pseudoknot, which resulted in a marked decrease in flexibility of its 2′-OH. Furthermore, the bases found in the loop opposing the pseudoknot fold presented various SHAPE results appealing for substitution. While the A11 base increases in flexibility with ligand addition, G12 undergoes first a slight destabilization before becoming markedly less flexible upon $preQ_1$ ligand addition, suggesting a crucial structural interaction. We substituted both bases for 2AP in order to monitor these two effects independently by their fluorescence response. Base A44 was further selected to detect the effects of ligand interaction on a distant loop. Lastly, we chose to substitute base A50 for 2AP because the 2′-OH of this base undergoes a 10-fold increased flexibility in the presence of $preQ_1$, as observed by SHAPE probing.

Fluorescence results for the addition of magnesium and $preQ_1$ to the 5 selected bases correlated well with the probing results (Figure 4C and Supporting Figure 3B, Supporting Information). However, for the first time we observed a major difference in the effect of magnesium and ligand on one of the bases. The adenine 50 was shown to have an increased 2′-OH flexibility only in the presence of the magnesium ions and $preQ_1$ ligand (Figure 4A and B). Interestingly, 2AP fluorescence data demonstrate a strong unstacking of the base in the presence of sole magnesium, while no further effect is observed upon $preQ_1$ addition (Figure 4C). This result suggests that the base A50 becomes unstacked upon magnesium binding in a way that does not render the 2′-OH accessible. This type of rare possibility was addressed in previous publications, suggesting that it is possible for a nucleotide to be constrained in a conformation that increases the reactivity of a specific 2′-OH.[26] In contrast, we observe the opposing effect with base A50, where the 2′-OH is constrained, while the adenine nucleobase is unstacked in the presence of magnesium. Direct interactions with 2′-OH for RNA recognition or folding have been reported in literature, for example, in GNRA tetraloops, RNase P RNA, and group I introns.[34−36] We therefore surmise, based on the SHAPE and 2AP fluorescence experiments, that the 2′-OH of the A50 base of the $preQ_1$cII aptamer is involved in a significant interaction that is severed in the presence of the $preQ_1$ ligand.

Importantly, when A50 is excluded from calculation, the correlation coefficients for the magnesium interaction are r = 0.89 and 1.00 in the presence of magnesium and $preQ_1$, corresponding to a very strong correlation. The fluorescence data further demonstrate that all selected positions present prominent fluorescence variations upon ligands addition (Figure 4C and Supporting Figure 3B, Supporting Information). The data support that these substitution positions, selected exclusively according to SHAPE reactivity and secondary structure, could be used for further structural dynamics studies of the $preQ_1$cII riboswitch, reporting timely events in the various important regions of the riboswitch structure.

Additionally, 2AP substitution monitors the stacking of the nucleobases, while SHAPE probing measures spatial disorder, more specifically at the 2′-OH position (Supporting Figure 4, Supporting Information).[11,24] The chemistry of the two experiments is different which can account for some of the discrepancies observed, such as differences in the effect range as well as the peculiar $preQ_1$cII A50 base data. This interesting result underlines that while this study demonstrates that SHAPE probing can be used to select proper labeling position for 2AP, these two methods do not monitor the same portion of the nucleoside, and in some cases, additional stimulating data can be acquired from comparison of the two experiments.

CONCLUSIONS

This study reports clear evidence of a direct correlation between 2′-OH reactivity probed by SHAPE using BzCN and the 2AP fluorescence of 26 various nucleotides in RNA structures. This correlation was further put to use to predict appropriate 2AP substitution sites in three highly structured RNA models: the SAM-II, addA, and $preQ_1$cII riboswitches. This approach offers the significant advantage of being the first straightforward procedure to predict 2AP substitution sites. This direct identification of substitution sites can theoretically be used on any RNA structure and can greatly improve the efficiency of 2AP labeling for both secondary/tertiary structural rearrangements monitoring techniques and the 2APFold approach.[23]

Currently, 2AP substitution sites are mainly being selected through careful consideration of secondary and tertiary structure of target RNAs. Although the availability of high-resolution structures has increased considerably in recent years, their impact on site selection for 2AP substitutions seems limited because these structures usually depict a RNA molecule in a single conformation, mainly after ligand binding, in the presence of high concentrations of metal ions. Therefore, while we get a glimpse at the final conformation of the nucleobases, prediction of dynamic positions for use in 2AP experiments was so far only achieved via educated guesses. In this context, the appeal of SHAPE, as well as other probing methods,[37,38] is in the fact that they allow insights into unfolded or partially folded structures, when performed in the absence of ligand and/or metal ions. SHAPE can also confirm or infirm the predicted secondary structure folding of a target RNA. We further demonstrated, in the current study, that SHAPE reactivity can be correlated with 2AP nucleobases fluorescence, leading to the direct selection of substitution sites for fluorescence-based assays. The correlations observed between data sets from SHAPE and 2AP fluorescence were always of positive values, highlighting that the direction of the effects of magnesium and ligand on the riboswitches are conserved between the two techniques (high SHAPE relative value correlates with high fluorescence relative value; low SHAPE with low fluorescence).

Our previous studies suggested, based on crystallographic data and 2AP fluorescence experiments, that a rather large number of nucleosides in a RNA (up to 10−15%)[23] can be used for the replacements by 2AP sensors without disturbance of the overall

fold, even in crucial and highly conserved tertiary structure regions. The high tolerance for 2AP substitutions is surprising at first sight. Although our findings here are based on a limited set with respect to RNA species, the tolerance can be well rationalized if high-resolution structures are available, as in the case of SAM-II and adenine riboswitches. Analysis of their X-ray crystal structures reveals that nucleosides tolerate 2AP substitutions provided that hydrogen bonding and nucleobase stacking patterns at the very positions are retained to a major extent. Taking that into account, the percentage of around 10% of nucleosides that are appropriate for 2AP substitutions becomes understandable. This rationale can support 2AP site selection (provided that a high-resolution structure is available) but will only lead to a subset of potential sites. More importantly, these substitutions might not necessarily result in a pronounced fluorescence response of the 2AP substitution, since the required change in nucleoside environment that is responsible for a broad 2AP fluorescence change remains concealed by a simple, static analysis of the RNA structure. The strength of the novel approach introduced here lies in the fact that the selection tool we use, namely SHAPE, is sensitive to changes in the nucleoside environment and therefore allows a more targeted approach for the selection of substitution sites. It is thus superior to site selection based on X-ray structures solely and provides the additional advantage of being a very fast method that can be performed in most biochemistry laboratory.

As a general remark on the possible influence of the nature of the RNA, we mention that the rationale for successful 2AP substitutions given above seems reliable for highly structured RNAs (such as riboswitches or ribozymes), while predictions for less structured RNAs might be more difficult. Nonetheless, the correlated results from SHAPE probing and 2AP fluorescence presented in the current study demonstrate that for all 26 2AP substitution positions tested, purines (A, G) and pyrimidine (U) alike, none interfered with the normal RNA folding detected on the wild-type sequence by probing. We feel that this conclusion succeeds in elevating the appeal of 2AP substitution methods for the measurements of structural folding and folding kinetics of RNA molecules.

MATERIAL AND METHODS

RNA Transcription for Chemical Probing. SAM-II, addA, and preQ$_1$cII RNAs of respectively 97, 98, and 85 nucleotides were synthesized using a pair of complementary oligonucleotides (IDT) including a T7 RNA promoter followed by the sequence of the RNA with flanking 5′ and 3′ linkers for reverse transcription. Following transcription at 37 °C for 2 h, phenol/chloroform extraction, and isopropanol precipitation, the RNA substrates were separated on a denaturing 8% polyacrylamide gel (90 min, 28 W) and visualized by ultraviolet shadowing. The corresponding bands were excised and then eluted from the gel by an overnight incubation in 0.1% SDS/0.5 M of ammonium acetate. The RNA was then precipitated with isopropanol, and the pellets were resuspended in nanopure water. The RNA substrates were then quantified by spectrophotometry and stored at −20 °C.

RNA 2′-Hydroxyl Acylation by Benzoyl Cyanide. Reaction mixtures containing T7-transcribed unlabeled RNA (5 pmol) with a 3′-end flanking sequence and 50 mM of MOPS at pH of 7.5 and 100 mM of KCl in the presence or absence of 2−5 mM of $MgCl_2$ and 5−10 μM of ligand (adenine, *S*-adenosylmethionine, or preQ$_1$) were heated at 65 °C for 2 min, cooled to 4 °C for 5 min, and incubated at 37 °C for 25 min in an Eppendorf Mastercycler personal (VWR). Following incubation, the control background reaction was treated with DMSO$_{ANH}$, while the probing reagent benzoyl cyanide (BzCN), dissolved in DMSO$_{ANH}$, was added to the probing reaction mixtures for a final concentration of 55 mM. The RNA was recovered by ethanol precipitation with sodium acetate and glycogen. The RNA samples were resuspended in 8 μL sterile water after centrifugation and stored at −20 °C.

Primer Extension. DNA primers (18 nt) were 5′-end labeled with γ^{32}P-ATP (Hartmann analytic) using T4 polynucleotide kinase (Fermentas) according to the manufacturer's instructions. Three μL of labeled DNA primer was added to 8 μL of RNA from BzCN 2′-hydroxyl acylation and allowed to anneal at 65 °C for 5 min, then incubated at 35 °C for 5 min, and cooled at 4 °C for 1 min in an Eppendorf Mastercycler personal. Eight μL of a mix containing 4 μL of 5× first strand buffer (250 mM of Tris-HCl at pH of 8.3, 375 mM of KCl, 15 mM of $MgCl_2$), 1 μL of 0.1 M DTT, 1 μL of 10 mM dNTPs mixture, and 2 μL of DMSO was then added to the reactions, followed by incubation at 61 °C for 1 min, addition of 0.4 μL of SuperScript III reverse transcriptase (Invitrogen), and further incubation at 61 °C for 10 min. Reactions were then stopped by addition of 1 μL of 4 N NaOH and incubation at 95 °C for 5 min. Radiolabeled cDNA strands were recovered by ethanol precipitation with sodium acetate and glycogen. The samples were resuspended in 8 μL of migration buffer (xylene cyanol, 97% formamide, 10 mM of EDTA) after centrifugation. Sequencing ladders were produced by adding 1 μL of 10 mM ddGTP or ddCTP in addition to the 8 μL of reaction mixture of unmodified RNA samples, prior to incubation at 61 °C. Electrophoresis on a 10% polyacrylamide gel for 95 min at 45 W was used to separate 300−500 cpm of the generated cDNA fragments. The gel was dried using a Vacuum-GelDryer (VWR) at 75 °C for 45−60 min. Following overnight exposition on a ^{32}P-sensitive phosphorscreen, the primer extension labeling was revealed by autoradiography. Band intensities visualized by gel electrophoresis were quantified using SAFA v.1.1 (Semi-Automated Footprinting Analysis). Data sets were normalized for loading variations and RT efficiency by dividing all intensities by the intensity of the last bases of primer extension. Final results for graphical representation were obtained by subtracting the DMSO$_{ANH}$ control background from the BzCN-probed reaction intensities. The data reported in tables is relativized for comparison by dividing each normalized probing value by the value of the initial riboswitch state probing (absence of magnesium and ligand; BzCN labeled lane on gels).

Solid-Phase RNA Synthesis. RNA oligonucleotides containing a 2AP nucleotide for fluorescence experiments were synthesized on Pharmacia Gene Assembler or Applied Biosystems instrumentations using 2′-*O*-TOM protected phosphoramidite nucleoside building blocks. RNA oligos were deprotected by using CH_3NH_2 in EtOH (8 M, 0.5 mL) and CH_3NH_2 in H_2O (40%, 0.5 mL) at room temperature for 6 h. After complete evaporation of the solution, the 2′-*O*-TOM protecting groups were removed by treatment with 315 mg tetrabutylammonium fluoride trihydrate (TBAF·3H_2O) in 1.0 mL of 1 M THF for at least 14 h at 37 °C. The reaction was quenched by addition of 1.0 mL of 1 M triethylammonium acetate at pH of 7.0. The solution was loaded on a GE Healthcare HiPrep 26/10 desalting column, and the crude RNA was eluted with H_2O. Analysis of oligonucleotides after deprotection was performed by anion-exchange chromatography on a Dionex DNAPac100 column at 80 °C (flow rate: 1 mL/min; eluant A: 25 mM of Tris-HCl at pH of 8.0, 6 M of urea; eluant B: 25 mM of Tris-HCl at pH of 8.0, 0.5 M of $NaClO_4$, 6 M of urea; gradient: 0−40% B in A within 30 min (<20 nt) or 0−60% B in A within 45 min (>20 nt); UV detection at 260 nm). Oligonucleotides were further purified on a semipreparative Dionex DNAPac100 column at 80 °C (Flow rate: 2 mL/min; gradient: Δ5−10% B in A within 20 min). Fractions containing the full-length RNA were loaded on a C18 SepPak cartridge (Waters/Millipore), washed with 0.1 M of $(Et_3NH)^+HCO_3^-$ and H_2O,

eluted with H_2O/CH_3CN 1:1, and lyophilized to dryness. The purified oligonucleotides were characterized by mass spectrometry on a Finnigan LCQ Advantage MAX ion trap instrumentation connected to an Amersham Ettan micro LC system.

Enzymatic Ligation of 2AP-Modified RNA. The 2AP containing RNAs of 52 nt (SAM-II), 71 nt (addA), and 56 nt (preQ$_1$cII) in lengths was prepared by splinted enzymatic ligation of two chemically synthesized fragments using T4 DNA ligase (Fermentas), as described in detail in refs 39−41. Briefly, 10 μM of each RNA fragment, 10 μM of a 25−30 nt DNA splint oligonucleotide (IDT), and a final ligase concentration of 0.5 U/μL in a total volume of 2 mL were incubated for 20 h at 37 °C. Analysis of the ligation reaction and purification of the ligation products was performed by anion exchange chromatography.

Fluorescence Measurements. All experiments were measured on a Cary Eclipse spectrometer (Varian) equipped with a peltier block and magnetic stirring device. For time course experiments, RNA samples were prepared in 0.5 μM concentration in a total volume of 125 μL with binding buffer (50 mM 3-(*N*-morpholino)propanesulfonic acid potassium salt (KMOPS) at pH of 7.0, 100 mM of KCl). The samples were preincubated for 15 min at 25 °C in the peltier controlled sample holder followed by manual injection of 2 μL aliquots. Spectra were recorded from 320−500 nm using the following instrumental parameters: excitation wavelength, 308 nm; emission wavelength, 372 nm; increments, 1 nm; scan rate, 120−300 nm/min; and slit widths, 10 nm. The results are graphically presented as the fluorescence variation as a function of time. The data reported in tables are relativized for comparison by dividing the mean value of each plateau by the mean value of the initial state plateau (absence of magnesium and ligand).

■ ASSOCIATED CONTENT

Supporting Information. 2AP fluorescence data and complete SHAPE probing quantifications. This material is available free of charge via the Internet at http://pubs.acs.org.

■ AUTHOR INFORMATION

Corresponding Author
ronald.micura@uibk.ac.at

Present Addresses
[†]Julius-Maximillians Universität, Institut für Molekulare Infektionsbiologie, Josef-Schneider-Straße 2, 97080 Würzburg, Germany.

■ ACKNOWLEDGMENT

This article is dedicated to Prof. Bernhard Kräutler on the occasion of his 65th birthday. M.F.S. thanks the European Molecular Biology Organization and European Commission FP7 (Marie Curie Actions, EMBOCOFUNDFP7, GA-2008-229685) for an EMBO long-term fellowship. Funding by the Austrian Science Foundation FWF (P21641, I317) and the Ministry of Science and Research (GenAU III "Non-coding RNAs"; project P0726-012-012) is acknowledged. M.F.S. and R.M. thank Ulrike Rieder for building up the ^{32}P laboratory and Ulrike Rieder and Veronika Schwarz for the preQ$_1$ ligand chemical synthesis.

■ REFERENCES

(1) Strobel, S. A.; Cochrane, J. C. *Curr. Opin. Chem. Biol.* **2007**, *11*, 636–643.
(2) Serganov, A.; Patel, D. J. *Nat. Rev. Genet.* **2007**, *8*, 776–790.
(3) Nudler, E.; Mironov, A. S. *Trends Biochem. Sci.* **2004**, *29*, 11–17.
(4) Zhou, X.; Wang, G.; Zhang, W. *Mol. Syst. Biol.* **2007**, *3*, 103–113.
(5) Inui, M.; Martello, G.; Piccolo, S. *Nat. Rev. Mol. Cell Biol.* **2010**, *11*, 252–263.
(6) Weigand, J. E.; Suess, B. *Appl. Microbiol. Biotechnol.* **2009**, *85*, 229–236.
(7) Wieland, M.; Hartig, J. S. *ChemBioChem* **2008**, *9*, 1873–1878.
(8) Batey, R. T.; Rambo, R. P.; Doudna, J. A. *Angew. Chem., Int. Ed. Engl.* **1999**, *38*, 2326–2343.
(9) Roth, A.; Breaker, R. R. *Annu. Rev. Biochem.* **2009**, *78*, 305–334.
(10) Schwalbe, H.; Buck, J.; Furtig, B.; Noeske, J.; Wohnert, J. *Angew. Chem., Int. Ed. Engl.* **2007**, *46*, 1212–1219.
(11) Jean, J. M.; Hall, K. B. *Proc. Natl. Acad. Sci. U.S.A.* **2001**, *98*, 37–41.
(12) Sinkeldam, R. W.; Greco, N.; Tor, Y. *Chem. Rev.* **2010**, *110*, 2579–2619.
(13) Law, S. M.; Eritja, R.; Goodman, M. F.; Breslauer, K. J. *Biochemistry* **1996**, *35*, 12329–12337.
(14) Sowers, L. C.; Fazakerley, G. V.; Eritja, R.; Kaplan, B. E.; Goodman, M. F. *Proc. Natl. Acad. Sci. U.S.A.* **1986**, *83*, 5434–5438.
(15) Means, J. A.; Simson, C. M.; Zhou, S.; Rachford, A. A.; Rack, J. J.; Hines, J. V. *Biochem. Biophys. Res. Commun.* **2009**, *389* (4), 616–621.
(16) Heppell, B.; Mulhbacher, J.; Penedo, J. C.; Lafontaine, D. A. *Methods Mol. Biol.* **2009**, *540*, 25–37.
(17) Lang, K.; Rieder, R.; Micura, R. *Nucleic Acids Res.* **2007**, *35*, 5370–5378.
(18) Rieder, R.; Lang, K.; Graber, D.; Micura, R. *ChemBioChem* **2007**, *8*, 896–902.
(19) Rieder, U.; Kreutz, C.; Micura, R. *Proc. Natl. Acad. Sci. U.S.A.* **2010**, *107*, 10804–10809.
(20) Haller, A.; Rieder, U.; Aigner, M.; Blanchard, S. C.; Micura, R. *Nat. Chem. Biol.* **2011**, *7*, 393–400.
(21) Heppell, B.; Lafontaine, D. A. *Biochemistry* **2008**, *47*, 1490–1499.
(22) Gilbert, S. D; Stoddard, C. D.; Wise, S. J.; Batey, R. T. *J. Mol. Biol.* **2006**, *359*, 754–768.
(23) Haller, A.; Soulière, M. F.; Micura, R. *Acc. Chem. Res.* **2011**, DOI: 10.1021/ar200035g.
(24) (a) Merino, E. J.; Wilkinson, K. A.; Coughlan, J. L.; Weeks, K. M. *J. Am. Chem. Soc.* **2005**, *127*, 4223–4231.(b) Weeks, K. M.; Mauger, D. M. *Acc. Chem. Res.* **2011**, DOI: 10.1021/ar200051h.
(25) Wilkinson, K. A.; Merino, E. J.; Weeks, K. M. *Nat. Protoc.* **2006**, *1*, 1610–1616.
(26) Low, J. T.; Weeks, K. M. *Methods* **2010**, *52*, 150–158.
(27) Mortimer, S. A.; Weeks, K. M. *J. Am. Chem. Soc.* **2007**, *129*, 4144–4145.
(28) Watts, J. M.; Dang, K. K.; Gorelick, R. J.; Leonard, C. W.; Bess, J. W., Jr.; Swanstrom, R.; Burch, C. L.; Weeks, K. M. *Nature* **2009**, *460*, 711–716.
(29) Gherghe, C. M.; Shajani, Z.; Wilkinson, K. A.; Varani, G.; Weeks, K. M. *J. Am. Chem. Soc.* **2008**, *130*, 12244–12245.
(30) Gilbert, S. D.; Rambo, R. P.; Van Tyne, D.; Batey, R. T. *Nat. Struct. Mol. Biol.* **2008**, *15*, 177–182.
(31) Serganov, A.; Yuan, Y. R.; Pikovskaya, O.; Polonskaia, A.; Malinina, L.; Phan, A. T.; Höbartner, C.; Micura, R.; Breaker, R. R.; Patel, D. J. *Chem. Biol.* **2004**, *11*, 1729–1741.
(32) Rieder, R., Ph.D. thesis, Leopold-Franzens Universität, Innsbruck, Austria, 2008.
(33) Meyer, M. M.; Roth, A.; Chervin, S. M.; Garcia, G. A.; Breaker, R. R. *RNA* **2008**, *14*, 685–695.
(34) Jucker, F. M.; Heus, H. A.; Yip, P. F.; Moors, E. H.; Pardi, A. *J. Mol. Biol.* **1996**, *264*, 968–980.
(35) Pan, T.; Loria, A.; Zhong, K. *Proc. Natl. Acad. Sci. U.S.A.* **1995**, *92*, 12510–12514.
(36) Pyle, A. M.; Cech, T. R. *Nature* **1991**, *350*, 628–631.
(37) Brunel, C; Romby, P. *Methods Enzymol.* **2000**, *318*, 3–21.
(38) Weeks, K. M. *Curr. Opin. Struct. Biol.* **2010**, *20*, 295–304.
(39) Lang, K.; Micura, R. *Nat. Protoc.* **2008**, *3*, 1457–1466.
(40) Rieder, R.; Höbartner, C.; Micura, R. *Methods Mol. Biol.* **2009**, *540*, 15–24.
(41) Höbartner, C.; Micura, R. *J. Am. Chem. Soc.* **2004**, *126*, 1141–1149.